

表① ABCD²スコア項目
(Johnston SC *et al*, 2007⁶⁾より改変引用)

項目	点数	スコア
A (age)	≥60 歳	1
B (blood pressure)	SBP≥140 mmHg または DBP≥90 mmHg	1
C (clinical features)	片側性脱力	2
	脱力を伴わない言語障害	1
	その他	0
D (duration)	≥60 分	2
	10~59 分	1
	<10 分	0
D (diabetes)	糖尿病	1
合計		

梗塞が続発することが知られており、最近では TIA のリスク層別分析がおこなわれている。英国でおこなわれた 4 つの大規模臨床試験の成績から TIA に続発して 14 日以内に脳梗塞を発症した例の 50%以上は、TIA 発症後 48 時間以内の発症であった。このことは TIA 治療の開始を 24~48 時間以内に迅速にスタートすべきという勧告の根拠になっている。Johnston ら⁴⁾は米国において救急部門で TIA と診断された 1,707 例の 11%もの患者が脳梗塞の診断で救急室に再受診しており、しかもその半分が最初の 2 日以内であったと報告し、注意を喚起した。Rothwell ら⁵⁾は、英国において TIA 後、脳梗塞を早期に発症する危険因子を分析し、年齢 60 歳以上、高血圧、発作時の臨床症状が半身の麻痺または言語障害、症状の持続時間が 10 分以上の項目のオッズ比が高く、それらの総点数が増加するごとに、7 日以内の早期の脳梗塞発症率が高くなることを報告した。これは Age (年齢)、Blood pressure (血圧)、Clinical feature (臨床的特徴)、Duration (持続時間)の頭文字をとって ABCD スコアと名付けられた。その後さらに Diabetes Mellitus (糖尿病)を加えて最初の 48 時間以内の脳梗塞リスクも最も良く予測するスコアとして改良されたものが ABCD²スコア⁶⁾⁷⁾である(表①)。TIA 研究のメタ解析²⁾では研究方法や対象、治療などがさまざまに結果に不均等性があるものの、救急の TIA 患者が専門医のいる脳卒中診療施設で救急治療を受けた研究⁸⁾⁹⁾では発症率が低いことが明らかになった。さらに ABCD²スコアの合計点数が高い例では、2, 7, 30, 90 日以内の脳梗塞発症の危険が累積的に高くなる⁶⁾(図①)。また入院中の患者であっても ABCD

スコアの低い例において入院中の 30 日以内の脳梗塞発症リスクと相関するとの報告¹⁰⁾や、たとえスコアが低くても 50%以上の頸動脈狭窄や心房細動例を含むハイリスク例が含まれていることなどが報告されている¹¹⁾。Oxford Vascular Study の TIA 患者 285 例のうち 29 例(10.2%)に 50%以上の頸動脈狭窄を認め、これらのなかで、7 日以内に脳梗塞を生じた例では ABCD スコア、ABCD²スコアが高い傾向にあった¹²⁾。また North America Symptomatic Carotid Endarterectomy Trial (NASCET) の TIA の既往を有する頸動脈高度狭窄(70~99%)に対しては、アスピリン投与の内科治療群では 7 日以内に 8.5%、90 日以内に 20%に同側の脳梗塞を生じており、頸動脈高度狭窄病変を伴う TIA の危険性が明らかになっている¹³⁾。最近の地域住民を対象とした TIA 研究では、50%以上の頸動脈狭窄を有する場合でも、頸動脈の血管評価や手術が遅れることで 14 日以内の脳梗塞発症頻度が約 20%にも達することが明らかになっている¹⁴⁾(図②)。これらのことから最近では頸動脈内膜剥離術(carotid endarterectomy: CEA)は、症状が軽症の場合には発症後 2 週間以内など、比較的早期に手術をおこなうことが最もメリットが大きいと勧められている¹⁵⁾。いかに早く専門医を受診し、頸動脈を含む早期評価をおこない、内科治療か外科治療かの適応を判断し、すみやかに治療が開始されるかが、転帰を左右する重要なポイントであることを示している。

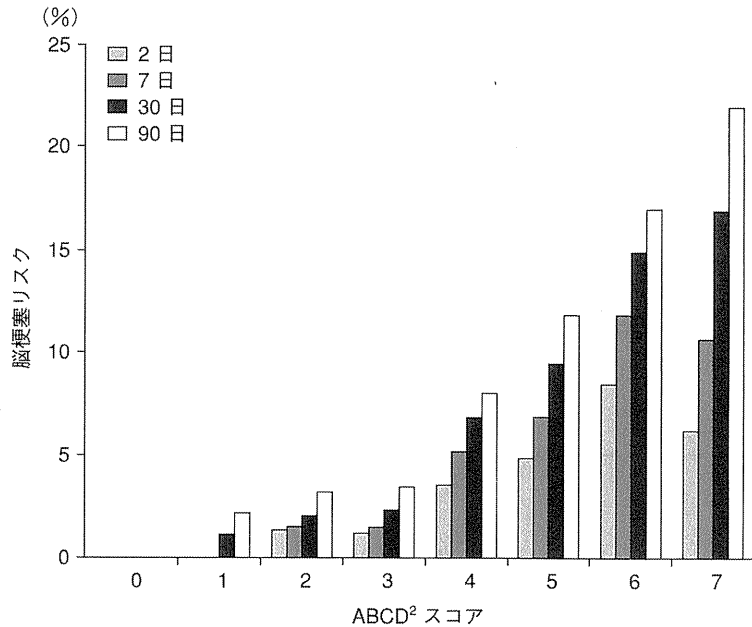


図1 ABCD²スコアからみた六つの臨床研究 4,799 例における TIA 患者の脳梗塞発症短期リスク (Johnston SC *et al*, 2007⁶⁾より引用)
 ■, ■, ■, □はそれぞれ TIA 後 2 日, 7 日, 30 日, 90 日以内の発症の累計リスク (%) を示している。

2 頸動脈病変が TIA を生じるメカニズム

大血管障害による脳梗塞では、一本の太い脳動脈領域における皮質梗塞として現れ、動脈硬化病巣の血管内閉塞または 50%以上の狭窄がみられる。このようなカテゴリーの脳梗塞には先行して TIA が現れることが多い。これらの虚血の機序は動脈硬化部位から末梢血管への artery-to-artery 塞栓または血行動態不全のいずれかと考えられている。これらの機序については必ずしも一つに断定でない場合が多いが、急性期の血流評価や梗塞巣の分布などからある程度の推察が可能である¹⁶⁾(図3: 症例の経過図と DWI 高信号病変)。

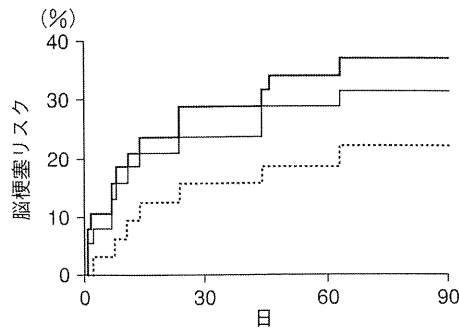
TIA の病態を考える場合、その発症機序を推察し、その病態や臨床病型を確かめる検査を迅速におこなうことが重要である。いわゆる large vessel disease (大血管病)に伴う TIA では脳卒中の発症リスクはそれぞれ 4%/7 日, 12.6%/30 日であるのに対し、ラクナ梗塞ではそれぞれ 0%, 2%と低かった¹⁷⁾。Large vessel disease を伴う TIA は全体の 17%であるのに、発症 7 日以内に発症した脳梗塞の 37%を占めている状況である。このように頭蓋外の大血管の動脈硬化が進展している例では、より早期からの評価と発症予防が必要である。発作当日や TIA 類

発例、ABCD スコアが高い例などは、ただちに入院のうえ、脳梗塞治療を開始したうえで、短期間で評価を完了することが推奨されている¹⁸⁾。その日のうちに脳と脳血管の画像検査 (MRI または CT) や頸部血管超音波検査、心電図、血液検査などをおこない、脳梗塞や血管病変の有無、心房細動の合併、糖尿病や凝固異常などを評価する。TIA は完成型脳梗塞に至る最終段階、「崖っぷち」予防段階とも呼ぶべき危険な状態で、市民への啓発が必要である¹⁹⁾。

3 頸動脈病変の評価

1) 頸動脈病変の非侵襲的スクリーニング (表2)

頸部血管超音波検査と MR 血管撮影または造影 CT 血管撮影が用いられる³⁾。頸部血管エコーは、費用対効果が良く、ベッドサイドでくり返し評価可能で、リアルタイムに動態画像として捉えられること、血流速度の計測が可能なことなど利点が多く、頸動脈病変評価の第一選択の検査機器といえる²⁰⁾。超音波検査については、発症早期に頸部および頭蓋内の中等度～高度狭窄病変を頸動脈超音波検査および経頭蓋ドプラで検出すれば、90 日後の脳卒中リスクが 3 倍高いことも示されている³⁾²¹⁾。



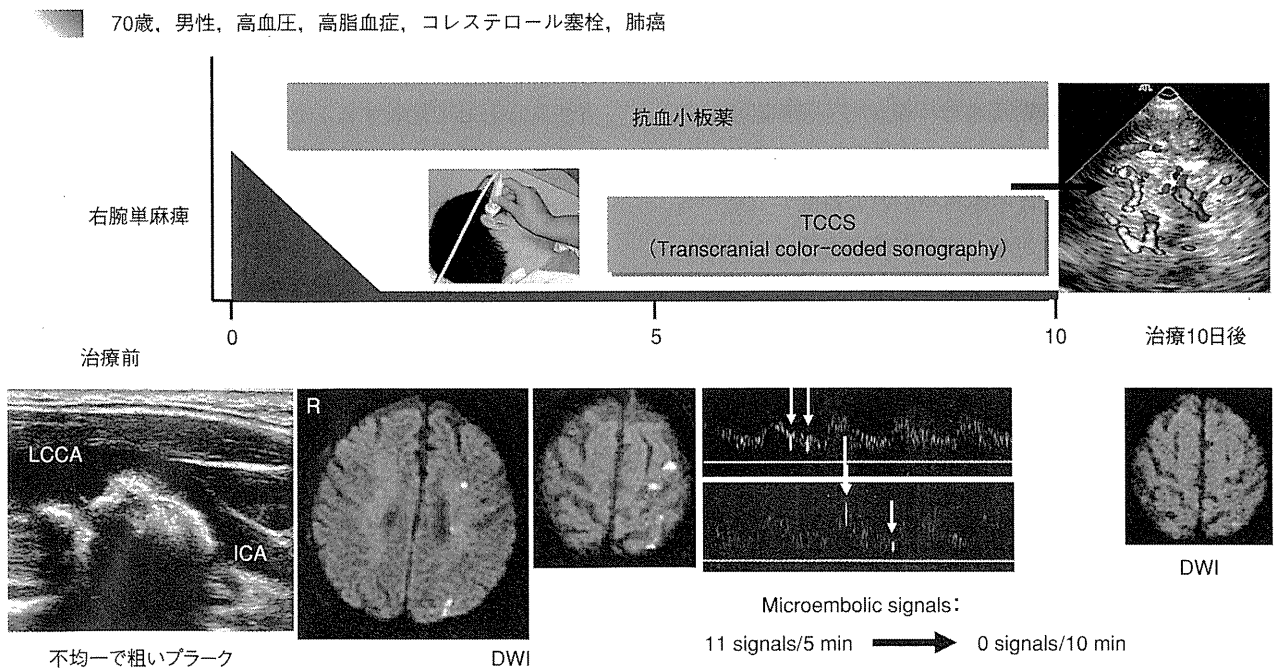
Numbers at risk	0	30	60	90
All recurrent stroke	38	27	22	19
Recurrent stroke after seeking medical attention	38	29	24	21
Recurrent stroke after seeking medical attention excluding carotid occlusions	32	27	23	20

図② 地域住民を対象とした Oxford Vascular study における TIA および minor stroke 患者の脳梗塞発症リスク (Johnston SC *et al*, 2007⁶⁾; Fairhead JF *et al*, 2005¹⁴⁾より改変引用)

太い実線は、症候性頸動脈狭窄 (≥50%) を伴う CEA 待機患者。細い実線は、TIA, minor stroke 患者が内科治療を開始前に脳梗塞を発症するリスク。破線は頸動脈の評価前に脳梗塞を発症し、その時点で頸動脈閉塞が明らかになった患者のリスク。

ただし技術には熟練を要し、現時点では必ずしもすべての脳卒中診療施設で検査可能といえる状況にはない。また検査上の難点として、内頸動脈の遠位部や著しい屈曲部位、高度な石灰化部分の評価が難しいことや正確な流速測定などには熟練を要することがあげられる。

一方、MR 血管造影は一定の検出力でルーチンにおこなうことができ、高度狭窄病変の検出において感度特異度 (92%, 72%) が高く、超音波検査 (88%, 76%) に勝っている²²⁾。しかし微細な内中膜の肥厚やプラーク、潰瘍、可動性病変の観察や局所の流速測定などは困難である。また軽度～中等度狭窄の評価は、超音波検査のほうが優れており、屈曲や磁場に影響する構造物の存在でアーチファクトが出現する。造影 CT 血管造影は三次元の画像で比較的正確な狭窄や構造が得られ、石灰化病変の評価に優れている。カテーテルを用いた脳血管造影と比較した研究²³⁾でも 70%以上の高度狭窄の陰性的中率は 100%と優れており、超音波検査、MR 血管造影と同様にスクリーニング検査の価値を有する。ただ大量の造影剤を使用するため、アレルギー歴のある場合や腎機能障害例では注意を要する。血行再建術を念頭においた頸



図③ 頸動脈高度狭窄を伴う TIA (70 歳, 男性). (Uchiyama S *et al*, 2009¹⁶⁾を改変引用)

TIA で緊急入院後に、頸部血管エコーで頸動脈高度狭窄合併が判明した。頭部 MRI 拡散強調画像では、左中大脳動脈領域に散在性の高信号域を認め、一部に脳梗塞を生じている。経頭蓋超音波検査では MES を検出した。

表② AHA/ASA 科学ステートメントにみる TIA 患者の頸部血管イメージングの推奨

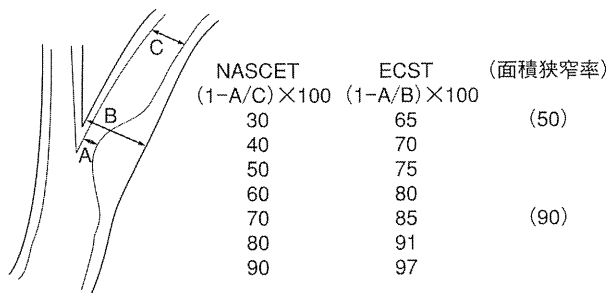
(Easton JD *et al*, 2009³⁾より改変引用)

頸動脈超音波検査は、TIA の原因診断のワークアップ、および頸動脈および椎骨動脈病変に対する手術、または血管内治療の可能性についてスクリーニングするうえで有用な検査である

従来の脳血管撮影は頸動脈内膜剝離術の狭窄度の正確な計測のゴールドスタンダードであり、術前の狭窄度測定には頸動脈超音波検査が推奨される。

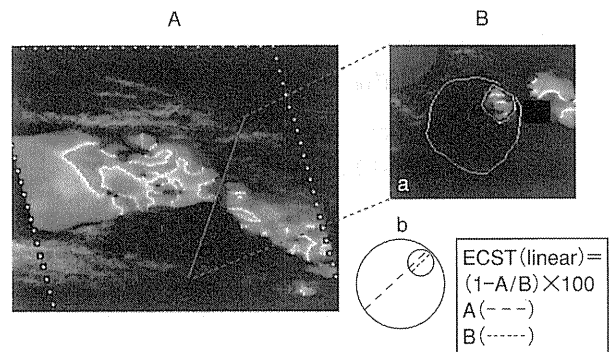
個々の患者において頸動脈超音波検査結果の信頼性が乏しく、かつ頸動脈内膜剝離術が考慮される場合には、大動脈から上行する血管評価には MRA または CTA が推奨される。

頸動脈超音波検査と MRA との結果が異なる場合や適応できない場合には、脳血管撮影検査が推奨される。



図④ 頸動脈狭窄測定法 NASCET と ECST の狭窄率の対比

(上床武史ほか, 2008²⁰⁾より改変引用)



図⑤ 頸動脈超音波検査カラードプラを用いた内頸動脈狭窄度測定の一例

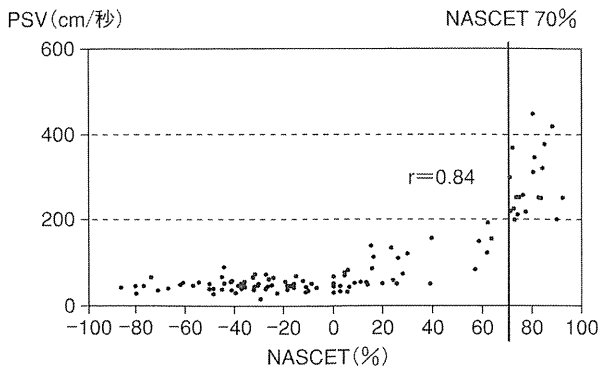
A: 長軸像 モザイク状の狭窄病変を認める。
B: 短軸像 ECST 法 83% の高度狭窄を示す。
(a: 面積表示, b: ECST 法表示)

動脈狭窄の精密な評価の場合は、現在でも頭頸部血管造影がゴールドスタンダードである²⁴⁾が、高度狭窄では血管造影時に約 1% を超える不可逆的な合併症が発症するとの報告²⁵⁾もあり、最近では頸動脈造影をおこなわずに、超音波検査と造影 CT 血管造影のみで CEA をおこなう施設もみられる。一般的にカテーテル血管造影を予定せずに CEA をおこなう場合は、狭窄度評価のエラーを避けるために二つの非侵襲的検査を施行し、同一所見を得ることが推奨されている³⁾。

2) 狭窄率の測定

頸動脈狭窄率の測定²⁰⁾については、径狭窄測定と面積狭窄測定があり、径狭窄については、狭窄評価が厳しい NASCET 法と外径との比較による ECST (European Carotid Surgery Trial) 法とがある。これらの測定法によって狭窄率が異なるために狭窄率の評価の際には測定

方法を合わせて記載することが重要である (図④, ⑤)。さらに高度狭窄部位では血流速度が上昇することから、逆に血流速度から狭窄率を推定する方法もある。これまでの報告から TIA など症候性脳卒中発作を生じ、CEA などの施行が推奨される NASCET 70% に匹敵する狭窄率の場合、対側や遠位部の影響がない場合には、収縮期最大流速 200 cm/s 以上とされている²⁶⁾(図⑥)。また遠位部の高度狭窄や閉塞の場合には、総頸動脈拡張末期血流速度が低下し、対側との比 (健側/患側) が 1.4 以上になることが知られている。九州医療センターでは、この他、面積狭窄率 90% 以上、径狭窄率 70% 以上を入院精査の目安としている。また、頸動脈ステントの実施基準の超音波検査で狭窄部の血流速度が 230 cm/s 以上などが一つの目安としてあげられている。これらの指標を駆使しながら TIA が生じた虚血側の頸動脈に臨床的意義のある病変があるかないかについて、早期に評価する。



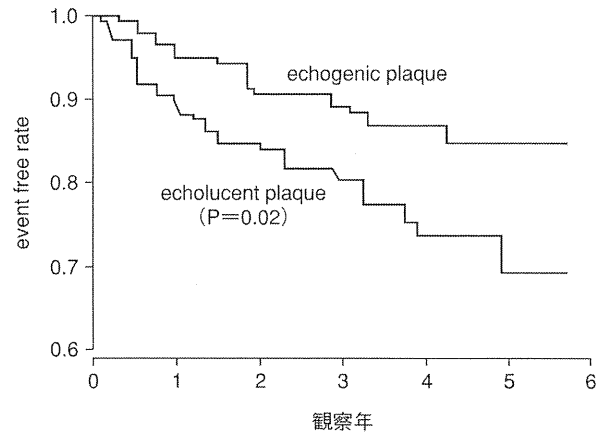
図⑥ 頸部血管エコーの血流速度と狭窄度の相関
(Koga M *et al*, 2001²⁶⁾より改変引用)

3) プラークの性状

狭窄率とともに狭窄部プラークの性状評価が重要である。輝度は低輝度(hypo-)、等輝度(iso-)、高輝度(hyper-)に分類され、低輝度病変は血液の輝度に近く、プラーク内出血や脆弱な粥腫病変を反映するとされており、脳梗塞のリスクと認識されている²⁷⁾(図⑦)。さらに潰瘍病変や可動性病変を伴うものも、将来の同側の脳梗塞の危険因子である。不安定プラークとは狭窄部の内皮に炎症がみられる、一部剥離や亀裂、潰瘍などがみられ、線維性皮膜が非常に薄く、脂質コア部分が大きく、脆弱なプラークを意味する²⁸⁾。ただ現時点ではプラークの性状に関して診療指針に明記するような臨床的な位置づけは定まっていない³⁾。

4) 微小栓子シグナルの検出

TIA をくり返す症例で、経頭蓋超音波検査をおこなうと微小栓子シグナル(microembolic signal: MES)を検出することがある。多くは不安定プラークで、剥離した内皮上や潰瘍病変内で凝集した血小板を中心とする微小栓子で、頭蓋内で自然に再開通していると考えられ、臨床的に応用されている。ただし症候を有する患者で検出感度が6%と低く、ルーチン検査としては推奨できない。これらの現象は血小板凝集能が亢進していることを意味しており、強力な抗血小板薬を投薬するなどの工夫ができる。Clopidogrel and Aspirin for Reduction of Emboli in Symptomatic Carotid Stenosis (CARESS) study²⁹⁾では、MESが検出された患者に対してアスピリン 100 mg 群とアスピリン 100 mg+クロピドグレル 300→75 mg 群とを比較したところクロピドグレル追加群ではMES検



図⑦ 頸動脈プラーク超音波輝度と脳梗塞発症の危険性
(Gronholdt ML *et al*, 2001²⁷⁾より改変引用)

低輝度プラークは、狭窄度や他の動脈硬化危険因子とは独立した同側の脳梗塞発症の危険因子であることが示された。

出患者数、時間あたりのMES検出頻度が有意に減少し、虚血発作の再発も少ない傾向がみられた。ただしMESについても現時点では診療指針に明記するような臨床的な位置づけは定まっていない³⁾。

4 | 全身血管リスクとしてのTIA患者の早期頸動脈評価

1) 頸動脈病変合併患者からみた全身合併症

TIA患者に遭遇した場合、脳循環や頸動脈病変の評価をもとに続発する脳梗塞を予防するとともに、全身の動脈硬化リスクを評価して長期の心血管イベントによる死亡やADL低下を予防することも同様に重要である。わが国において50%以上の頸動脈狭窄病変患者を1,000例以上集計して観察研究をおこなったJapan Carotid Atherosclerosis Study (JCAS) 研究³⁰⁾でTIA患者の占める割合は17%であった。そのJCAS患者の動脈硬化性疾患の合併率をみると、同年代の高齢者に比べて、高血圧、糖尿病、高脂血症などが著しく高く、各疾患の合併率が高く、しかも多重リスクである場合が多い。全世界で60,000例以上の患者を集計して心血管イベントの観察研究をおこなっているReduction of Atherothrombosis for Continued Health (REACH) 研究でもTIA患者は頸動脈病変の合併率が高く、冠動脈疾患患者と同様のプロフィールを有していた³¹⁾。

2) 冠動脈疾患の有病率

欧米の小規模研究では TIA または脳卒中患者において心筋虚血誘発試験で 20～40% に無症候性の心筋虚血がみられる³²⁾。TIA を含む急性虚血性脳卒中の臨床試験の短期のリスクに関するデータでも 90 日以内に 2% 前後の心臓関連死がみられる。脳卒中または TIA 患者に対する精密検査で著しい頸動脈病変を認めた場合は無症候性の冠動脈疾患を有する頻度が高いことが指摘されている。Urbinati ら³³⁾ は心臓症状がみられなかった 106 例の CEA 患者の TI-201 心筋血流イメージングで 27 例 (25%) の異常所見を認め、Chimowitz ら³⁴⁾ も心臓症状を有さない患者に対してアデノシンまたは運動負荷による TI-201 心筋イメージングをおこない、頸部頸動脈狭窄あるいは頸部と頭蓋内の双方の狭窄があった 22 例中 13 例 (60%) に心筋イメージングの異常所見を認めたとしている。Okin ら³⁵⁾ は心血管系の疾患の臨床所見がない 204 例の無症候性頸動脈病変患者に頸動脈超音波検査と運動負荷心電図試験をおこなったところ、頸動脈に動脈硬化所見のみられた患者では 50% に運動誘発性心筋虚血がみられ、頸動脈病変のない例 (17%) と比較して有意に高かったと報告している。また Framingham Study のデータ³⁶⁾ では頸動脈雑音がみられる例ではみられない例にくらべて有意に心筋梗塞と血管障害による死亡リスクが高いことが示されている。20% 前後に冠動脈病変の合併もあり、将来の心血管病の発症の危険もあることから、早期に頸動脈病変および全身の動脈硬化リスク因子の評価をおこない、嚴重に危険因子を管理していくことが求められる。

3) 頸動脈病変を有する患者の冠動脈疾患のリスク

頸部頸動脈を含む主要脳血管の動脈硬化がみられる TIA または虚血性脳卒中患者では、その他の原因の脳卒中にくらべて末梢血管疾患の頻度が高く、運動負荷試験での陽性率が高かった。運動負荷試験の独立した危険因子は、喫煙、頸動脈または頭蓋内動脈の動脈硬化であった。これらのことから虚血性脳卒中または TIA の患者はすべて心血管系リスクについて包括的な評価を受けることが勧告され³⁷⁾、頸動脈疾患患者は未確認の冠動脈疾患が存在する可能性が高いため、心血管系リスクが高く、著しい頸動脈疾患があり脳虚血の症状を呈する患者に対しては、冠動脈疾患の非侵襲的検査を考慮することが勧

告されている。しかし、ラクナ梗塞患者では脳卒中発症後早期の心臓障害による死亡率や心臓リスクは低いといわれている³⁸⁾。また大部分の患者では脳卒中の発現後、短期間に心臓障害が発現したり、これにより死に至る率が比較的低いため、脳卒中の急性期には心臓検査をおこなうべきではない。CEA 施行前に通常の冠動脈疾患検査をおこなうことは推奨していないが、動脈硬化のリスクプロフィールから高リスクとされるサブグループについては、冠動脈疾患検査をおこなうことは賢明と考えられる。事実、九州医療センターで CEA を施行した連続 200 例における冠動脈病変合併率は 37.5% と高く、その半数が左主幹動脈病変または 3 枝病変と重度であった³⁹⁾。つまり TIA 患者に対しては、その機序を明らかにし、さらに、頸動脈疾患の有無と重症度を評価することが勧められる。それによって未検出の心疾患に関するリスクを定量化し、脳卒中の二次予防戦略を決定するうえで有用な情報が得られるのである³⁷⁾。このようにアテローム血栓性脳梗塞でとりわけ頸動脈病変を合併する場合には全身血管病としての対処が必要であることは欧米で早くから指摘されている。九州医療センターにおける無症候性頸動脈狭窄患者の長期予後の検討でも、心筋梗塞の発症率は脳梗塞発症率とほぼ同等であり、死亡例も年率 4% 前後と少なくない⁴⁰⁾。

おわりに

TIA への治療は単に、抗血小板薬の外来処方だけでは不十分である。TIA を引き起こす基盤に、動脈硬化病変や悪い生活習慣があり、これらを管理是正する生活習慣の改善、食事療法や併存症の治療をあわせておこなうことが重要である。とくに禁煙の徹底と適正体重の維持、適度な運動、高血圧、糖尿病の治療、高コレステロール血症にはスタチンを中心とした薬物療法が奨められる¹⁾。また頸動脈病変を有する TIA 患者ではしばしば虚血性心疾患、閉塞性動脈硬化症 (末梢動脈疾患) を合併しており、全身のアテローム血栓症を伴っていることから全身血管病として広い視野で対処する必要がある¹⁾⁸⁾⁹⁾⁴⁰⁾。生活習慣病に対する治療意識の低い患者には、この発作を契機に本気で予防を心がけるよう指導するべきである。TIA を契機に検出される頸動脈狭窄症は多くの動脈硬化危険因子のうえに成り立っており、長期的にみると脳卒

中のみならず他臓器の疾患で日常生活の質を低下させ、死亡することもある病態である。その治療の究極の目標は、健康寿命の延伸と生活の質の改善にあることを念頭におくことが大切である。血管内治療や CEA の目標は、狭窄部の安易な拡張や血管の整形にとどまってはならない¹⁾⁴⁰⁾。内科治療の目標もより広い視野のチーム医療で、他の併存疾患の転帰に及ぼす影響を含めて長期成績を検証し、健康寿命の延伸と生活の質の改善のための統合的な治療方針を立てて進んでいく必要がある。

●文 献●

- 岡田靖：頸部頸動脈狭窄症の内科治療。医学のあゆみ **228**：809-815, 2009
- Giles MF *et al*：Risk of stroke early after transient ischemic attack：a systemic review and metaanalysis. *Lancet Neurol* **6**：1063-1072, 2007
- Easton JD *et al*：Definition and evaluation of transient ischemic attack. A scientific statement for healthcare professionals from the American Heart Association/American Stroke Association Stroke Council；Council on cardiovascular surgery and anesthesia；Council in cardiovascular radiology and intervention；Council on cardiovascular Nursing；and the interdisciplinary council on peripheral vascular disease. The American Academy of Neurology Affirms the value of this statement as an educational tool for neurologists. *Stroke* **40**：2276-2293, 2009
- Johnston SC *et al*：Short-term prognosis after emergency department diagnosis of TIA. *JAMA* **284**：2901-2906, 2000
- Rothwell PM *et al*：A simple score (ABCD) to identify individuals at high early risk of stroke after transient ischaemic attack. *Lancet* **366**：29-36, 2005
- Johnston SC *et al*：Validation and refinement of scores to predict very early stroke risk after transient ischemic attack. *Lancet* **369**：283-292, 2007
- Rothwell PM *et al*：Recent advances in management of transient ischaemic attacks and minor ischaemic strokes. *Lancet Neurol* **5**：323-331, 2006
- Rothwell PM *et al*：Effect of urgent treatment of transient ischaemic attack and minor stroke on early recurrent stroke (EXPRESS study)：a prospective population-based sequential comparison. *Lancet* **370**：1432-1442, 2007
- Lavalley PC *et al*：A transient ischaemic attack clinic with round-the-clock access (SOS-TIA)：feasibility and effects. *Lancet Neurol* **6**：940-941, 2007
- Tsivgoulis G *et al*：Validation of the ABCD score in identifying individuals at high early risk of stroke after a transient ischemic attack. A hospital-based case series study. *Stroke* **37**：2892-2897, 2006
- Cucchiara BL *et al*：Is the ABCD score useful for risk stratification of patients with acute transient ischemic attack? *Stroke* **37**：1710-1714, 2006
- Koton S *et al*：for the Oxford Vascular Study：Performance of the ABCD and ABCD² scores in TIA patients with carotid stenosis and atrial fibrillation. *Cerebrovasc Dis* **24**：232-235, 2007
- Barnett HJM *et al*：Benefit of carotid endarterectomy in patients with symptomatic moderate or severe carotid stenosis. North American Symptomatic Carotid Endarterectomy Trial Collaborators. *N Engl J Med* **339**：1415-1425, 1998
- Fairhead JF *et al*：Population-based study of delays in carotid imaging and surgery and the risk of recurrent stroke. *Neurology* **65**：371-375, 2005
- Bond R *et al*：Systemic review of the risks of carotid endarterectomy in relation to the clinical indication for and timing of surgery. *Stroke* **34**：2290-2303, 2003
- Uchiyama S *et al*：New concepts of treatment for TIA as a medical emergency (Round table discussion). *International Review of Thrombosis* **4**：5-21, 2009
- Lovett JK *et al*：Early risk of recurrence by subtype of ischemic stroke in population-based incidence studies. *Neurology* **62**：569-573, 2004
- Johnston SC *et al*：National Stroke Association guidelines for the management of transient ischemic attacks. *Ann Neurol* **60**：301-303, 2006
- 岡田靖：脳卒中の予防と治療最前線。日経健康セミナー、日本経済新聞(夕刊)2009年8月7日号, 6, 2009
- 上床武史ほか：頸動脈狭窄症の診断。心臓 **40**：4-11, 2008
- Purroy F *et al*：Usefulness of urgent combined carotid/transcranial ultrasound testing in early prognosis of TIA patients. *Med Clin (Barc)* **126**：647-650, 2006
- Buskens E *et al*：Imaging of carotid arteries in symptomatic patients；cost-effectiveness of diagnostic strategies. *Radiology* **233**：101-112, 2004
- Josephson SA *et al*：Evaluation of carotid stenosis using CT angiography in the initial evaluation of stroke and TIA. *Neurology* **63**：457-460, 2004
- Willinsky RA *et al*：Neurologic complication of cerebral angiography；prospective analysis of 2899 procedures and review of the literature. *Radiology* **41**：204-210, 2000
- Committee for the Asymptomatic Carotid Atherosclerosis Study：endarterectomy for asymptomatic carotid artery stenosis. *JAMA* **273**：1421-1428, 1995
- Koga M *et al*：Diagnosis of internal carotid artery stenosis greater than 70% with power Doppler duplex

- ultrasonography. *AJNR Am J Neuroradiol* **22** : 413-417, 2001
- 27) Gronholdt ML *et al* : Ultrasonic echolucent carotid plaques predict future strokes. *Circulation* **104** : 68-73, 2001
- 28) Nighoghossian N *et al* : The vulnerable carotid artery plaque. Current imaging method and new perspectives. *Stroke* **36** : 2764-2772, 2005
- 29) Markus HS *et al* : Dual antiplatelet therapy with clopidogrel and aspirin in symptomatic carotid stenosis evaluated using Doppler embolic signal detection : the Clopidogrel and Aspirin for Reduction of Emboli in Symptomatic Carotid Stenosis (CARESS) trial. *Circulation* **111** : 2233-2240, 2005
- 30) 遠藤俊郎ほか : 頸動脈高度狭窄病変の本邦の現状 ; JCAS から. *脳卒中* **27** : 492-497, 2005
- 31) Rother J *et al* : Risk factor profile and management of cerebrovascular patients in the REACH registry. *Cerebrovasc Dis* **25** : 366-374, 2008
- 32) Giles MF *et al* : Risk of early death after transient ischaemic attack : a systematic review and meta-analysis. *Lancet Neurol* **6** : 1063-1072, 2007
- 33) Urbinati S *et al* : Frequency and prognostic significance of silent coronary artery disease in patients with cerebral ischemia undergoing carotid endarterectomy. *Am J Cardiol* **69** : 1166-1170, 1992
- 34) Chimowitz MI *et al* : Frequency and severity of asymptomatic coronary artery disease in patients with different causes of stroke. *Stroke* **28** : 941-945, 1997
- 35) Okin PM *et al* : Relation of exercise induced myocardial ischemia to cardiac and carotid structure. *Hypertension* **30** : 1382-1388, 1997
- 36) Wolf PA *et al* : Asymptomatic carotid bruit and risk of stroke. the Framingham Study. *JAMA* **245** : 1442-1445, 1981
- 37) Adams RJ *et al* : Coronary risk evaluation in patients with transient ischemic attack and ischemic stroke. A scientific statement for healthcare professionals from the stroke council and the council on clinical cardiology of the American Heart Association/American Stroke Association. *Circulation* **108** : 1278-1290, 2003
- 38) Longstreth WT Jr *et al* : Frequency and predictor of stroke death in 5888 participants in Cardiovascular Health Study. *Neurology* **56** : 368-375, 2001
- 39) Shimada T *et al* : Prediction of coronary artery disease in patients undergoing carotid endarterectomy. *J Neurosurg* **103** : 593-596, 2005
- 40) 岡田靖ほか : 無症候性頸動脈狭窄症 ; 進歩する内科治療. *脳と循環* **14** : 139-145, 2009

おかだ・やすし

岡田 靖 国立病院機構九州医療センター脳血管内科, 統括診療部長

1957年, 福岡県生まれ。

1982年, 九州大学医学部卒業, 九大第二内科研修医。1984年, 国立循環器病センター内科脳血管部門レジデント。1992~94年, 米国スクリプス研究所客員研究員。1994年 国立病院九州医療センター脳血管内科医長。1999~01年 厚生省九州地方医務局医療課長。2004年より現職。専門は, 脳卒中急性期の内科治療, 全身血管病としての脳血管障害医療。研究テーマは, 頸動脈病変, TIA・minor stroke の臨床的研究。趣味は, 親しき仲間との宴・イベント企画, 縁ある街への小旅行。夢は, 脳血管内科が全国に普及し, 脳血管障害に対する市民・学生教育, 医療が充実し, 臨床研究が発展し, 脳卒中が撲滅されること。

症例報告

中大脳動脈狭窄に起因する一過性脳虚血発作に対するシロスタゾール(プレタール)使用経験

Yasaka Masahiro
矢坂 正弘Sakima Kunihiro
崎間 邦洋Okada Yasushi
岡田 靖*

はじめに

左中大脳動脈狭窄に起因する一過性脳虚血発作に対してシロスタゾールを投与し、症状の軽快とともに狭窄病変の改善が認められた症例を経験したので、文献的考察を加えて報告する。

症例提示

症例：75歳，女性。

既往歴：72歳時より高血圧を指摘され，近医にて内服加療を受けていた。

嗜好：喫煙歴なし，機会飲酒。

家族歴：脳卒中なし，他に特記事項なし。

現病歴：2006年某月某日(第1病日)11時30分，電話中に言葉が出なくなるとともに右上肢の脱力を自覚し10分で軽快。近医受診し入院，オザグレルナトリウム点滴静注(80 mgを2回/日)，アスピリン100 mg，プラバスタチン(10 mg/日)，ロサルタン(25 mg/日)の内服開始。翌日(第2病日)退院し内服薬を継続した。第8病日に右上肢の脱力発作が再発し，近医再入院，MRIとMRA検査を施行し，左中大脳動脈狭窄を指摘され，降圧薬が中止され，ヘパリン投与が開始された。第10病日に精査加療を目的に当科へ転院。

治療経過：入院時，意識清明で高次脳機能障害なし。脳神経系は正常で，運動・感覚・深部腱反射に異状はみられず，失調もなかった。拡散強調画像を含む頭部

MRI検査では明確な新鮮および陳旧性脳梗塞を認めなかったが，MRA検査と脳血管撮影検査で左中大脳動脈高度狭窄を認めた(図1)。同病変に伴う一過性脳虚血発作と診断し，ヘパリン(1万単位/日)とオザグレルナトリウムを点滴静注し，経口薬としてアスピリン(100 mg/日)にシロスタゾール(100 mg/日)を追加した。左中大脳動脈領域の血管反応性は11.5%とやや低下していたものの，基礎血流(46 mL/min/100 g)は保たれていた。入院中に再発作はみられず，退院し経過観察の方針となった。退院後2009年まで経過を観察し，一過性脳虚血発作の再発や脳梗塞はみられなかった。発作1年後の2007年に施行したMRAで狭窄病変の改善を認めた(図2)。同病変に壁不正は残存しているものの，2009年まで再狭窄はみられなかった。

考察

本症例は高血圧を基盤として左中大脳動脈狭窄を呈し，同狭窄病変からの塞栓性機序に基づく一過性脳虚血発作と推察される。抗血小板薬のアスピリンや内膜保護作用を有するスタチン製剤のプラバスタチン投与下でも発作を繰り返し，シロスタゾール追加以後，発作が停止したことから，シロスタゾールの栓子形成抑制による一過性脳虚血発作予防効果が発揮されたものと推察される。さらに，狭窄病変が1年後の観察で改善している点は特筆に値する。韓国で行われたTOSSにおいても，アスピリンとシロスタゾール投与で症候性頭蓋内狭窄病変の改善が報告されている¹⁾。狭窄病変改善の機序として，シロスタゾールが有している抗

*国立病院機構九州医療センター脳血管センター脳血管内科

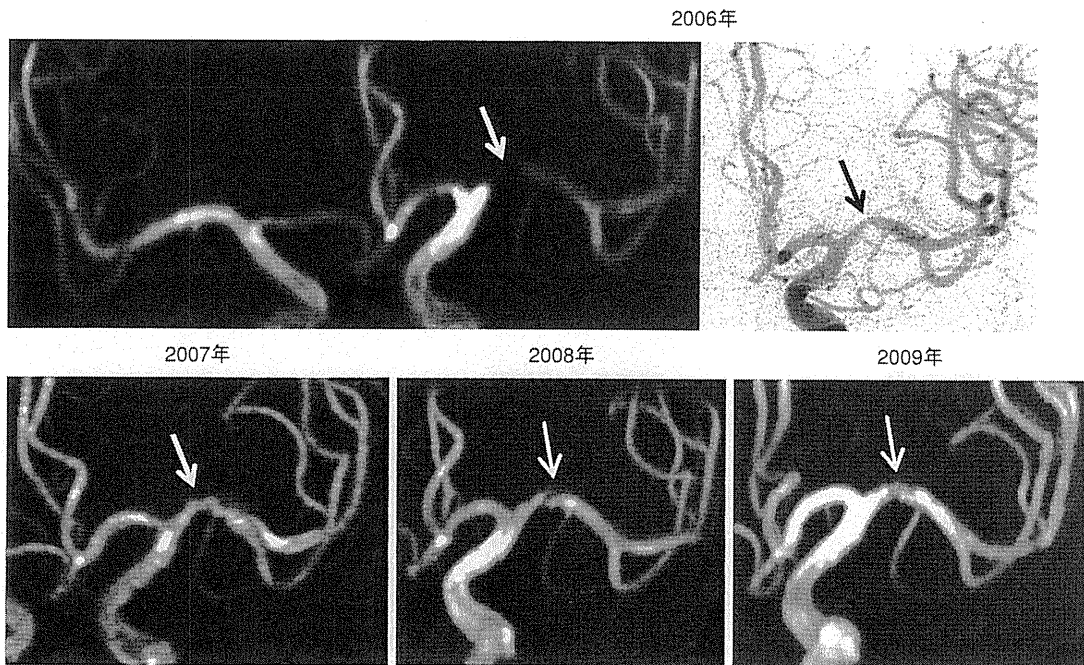


図1 頭蓋内狭窄病変の推移

上段：一過性脳虚血発作発症時のMRAと脳血管造影検査所見。左中大脳動脈に狭窄病変を認める。
下段：その後の頭部MRA検査所見。狭窄病変の改善を認める。

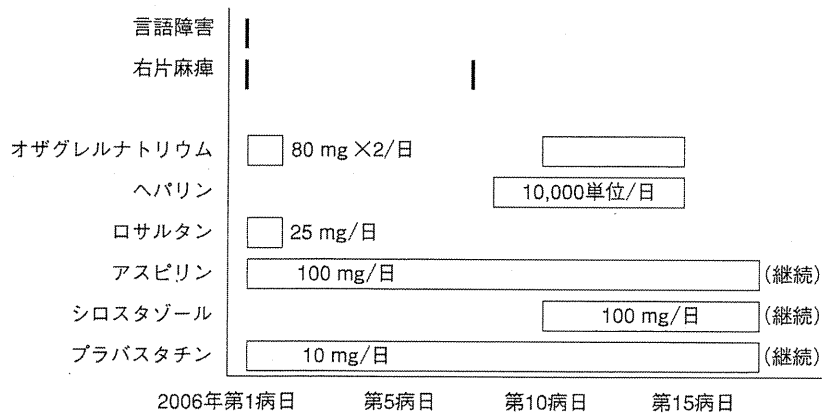


図2 発作と治療経過

シロスタゾール追加後、一過性脳虚血発作はみられなくなった。

血小板作用に加えての血管拡張作用や血管内膜機能改善作用が推察されている。もちろん、高血圧に伴う解離機序による狭窄病変の変化も否定できないが、TOSSでアスピリン単独群より有意に改善したことから、何らかの狭窄病変改善作用を有するものと推察される。本邦でも、症候性頭蓋内動脈狭窄進展抑制効果をアスピリン群とアスピリン、シロスタゾール併用群を対比するCATHARSIS研究²⁾が進められており、その結果が待たれる。

文献

- 1) Kwon SU, Cho YJ, Koo JS, et al : Cilostazol prevents the progression of the symptomatic intracranial arterial stenosis : the multicenter double-blind placebo-controlled trial of cilostazol in symptomatic intracranial arterial stenosis. Stroke 2005 ; 36 : 782-786.
- 2) Uchiyama S, Nakamura T, Yamazaki M, et al : New modalities and aspects of antiplatelet therapy for stroke prevention. Cerebrovasc Dis 2006 ; 21 (Suppl 1) : 7-16.

Note: This copy is for your personal, non-commercial use only. To order presentation-ready copies for distribution to your colleagues or clients, contact us at www.rsna.org/rsnarights.

Brain Temperature Measured by Using Proton MR Spectroscopy Predicts Cerebral Hyperperfusion after Carotid Endarterectomy¹

Toshiyuki Murakami, MD
Kuniaki Ogasawara, MD
Yoshichika Yoshioka, PhD
Daiya Ishigaki, MD²
Makoto Sasaki, MD
Kohsuke Kudo, MD
Kenta Aso, MD
Hideaki Nishimoto, MD
Masakazu Kobayashi, MD
Kenji Yoshida, MD
Akira Ogawa, MD

Purpose:

To determine whether brain temperature measured by using preoperative proton magnetic resonance (MR) spectroscopy could help identify patients at risk for cerebral hyperperfusion after carotid endarterectomy (CEA).

Materials and Methods:

Institutional review board approval and informed consent were obtained. Acquisition of proton MR spectroscopic data by using point-resolved spectroscopy without water suppression was performed before CEA in the bilateral cerebral hemispheres of 84 patients with unilateral internal carotid artery stenosis ($\geq 70\%$) and without contralateral internal carotid artery steno-occlusive disease. Brain temperature was calculated from the chemical shift difference between water and *N*-acetylaspartate signals at proton MR spectroscopy. Cerebral blood flow (CBF) was also measured by using single photon emission computed tomography and *N*-isopropyl-*p*-[¹²³I]-iodoamphetamine before and immediately after CEA and on the 3rd postoperative day. The relationship between each variable and the development of post-CEA hyperperfusion (CBF increase $\geq 100\%$ compared with preoperative values) was evaluated with univariate statistical analysis followed by multivariate analysis.

Results:

A linear correlation was observed between preoperative brain temperature difference (the value in the affected hemisphere minus the value in the contralateral hemisphere) and increases in CBF immediately after CEA ($r = 0.763$ and $P < .001$) when the preoperative brain temperature difference was greater than 0. Cerebral hyperperfusion immediately after CEA was observed in nine patients (11%). Elevated preoperative brain temperature difference was the only significant independent predictor of post-CEA hyperperfusion. When elevated brain temperature difference was defined as a marker of hemodynamic impairment in the affected cerebral hemisphere, use of preoperative brain temperature difference resulted in 100% sensitivity and 87% specificity, with a 47% positive predictive value and a 100% negative predictive value for the prediction of post-CEA hyperperfusion. Hyperperfusion syndrome developed on the 3rd and 4th postoperative days in two of the nine patients who exhibited hyperperfusion immediately after CEA.

Conclusion:

Brain temperature measured by using preoperative proton MR spectroscopy may help identify patients at risk for post-CEA cerebral hyperperfusion.

¹ From the Department of Neurosurgery (T.M., K.O., D.I., K.A., M.K., K.Y., A.O.) and Advanced Medical Research Center (Y.Y., M.S., K.K., H.N.), Iwate Medical University, 19-1 Uchimarui, Morioka 020-8505, Japan. Received May 27, 2009; revision requested July 15; revision received September 18; accepted October 7; final version accepted March 30, 2010. Supported in part by Core Research for Evolutional Science and Technology of Japan Science and Technology Agency. Address correspondence to K.O. (e-mail: kuogasa@iwate-med.ac.jp).

² Current address: Department of Biofunctional Imaging, Immunology Frontier Research Center, Osaka University, Osaka, Japan.

Cerebral hyperperfusion after carotid endarterectomy (CEA) is defined as a substantial increase in ipsilateral cerebral blood flow (CBF) after surgical repair of carotid stenosis that is well above the metabolic demands of brain tissue (1,2). Cerebral hyperperfusion syndrome after CEA is a complication of cerebral hyperperfusion that is characterized by unilateral headache, face and eye pain, seizure, and focal symptoms that occur secondary to cerebral edema or intracerebral hemorrhage (1–4). Although the incidence of intracerebral hemorrhage is relatively low (0.4%–1.8%), the prognosis for patients with this condition is poor (1,5–9). In addition, results of recent studies (10–12) have demonstrated that post-CEA hyperperfusion, even when asymptomatic, leads to postoperative cortical neural damage and subsequent cognitive impairment.

Risk factors for cerebral hyperperfusion include long-standing hypertension, high-grade carotid stenosis, poor collateral blood flow, and contralateral carotid occlusion, which are all associated with impairments in cerebral hemodynamic reserve (13). Furthermore, a rapid restoration of normal perfusion pressure after CEA may result in hyperperfusion in regions of the brain in which autoregulation is impaired because of chronic ischemia. This hypothesis is similar to the “normal perfusion pressure breakthrough” theory described by Spetzler et al (14) and is consistent with observations by several

investigators that decreased cerebrovascular reactivity to acetazolamide or elevated cerebral blood volume is a significant predictor of post-CEA hyperperfusion (15–18).

Magnetic resonance (MR) spectroscopy of the human brain yields a spectrum that includes a large water peak, as well as proton peaks related to *N*-acetylaspartate (NAA), creatines, and cholines (19–22), and human brain temperature (BT) can be calculated noninvasively and accurately from the chemical shift difference between water and NAA, choline, or creatine signals (19–22). In healthy humans, BT is determined by the balance between heat produced by cerebral energy turnover and heat removal (23). Because heat removal is primarily dependent on CBF (23), reduced cerebral perfusion relative to cerebral metabolism, termed “misery perfusion,” in patients with acute or chronic cerebral ischemia may indicate decreased central heat removal (ie, higher BT) (22,24). This is supported by observations from a recent study (24) that revealed that BT as measured with proton MR spectroscopy enabled detection of elevated cerebral blood volume and elevated oxygen extraction fraction with high sensitivity and specificity in patients with chronic unilateral major cerebral artery steno-occlusive disease.

The purpose of the present study was to determine whether BT measured by using preoperative proton MR spectroscopy could help identify patients at risk for cerebral hyperperfusion after CEA.

Materials and Methods

Patient Population

Between August 2008 and April 2009, 84 patients (74 men and 10 women)

Implication for Patient Care

- Brain temperature measured noninvasively by using proton MR spectroscopy predicts the development of cerebral hyperperfusion after carotid endarterectomy.

with unilateral internal carotid artery (ICA) stenosis ($\geq 70\%$) and good residual function (modified Rankin disability scale score, 0, 1, or 2) underwent CEA. All 84 patients were prospectively enrolled in the present study. Mean patient age was $67.5 \text{ years} \pm 7.6$ (standard deviation) ($67.4 \text{ years} \pm 7.5$ in men, $68.3 \text{ years} \pm 8.2$ in women), with a range of 47–82 years (47–82 years in men, 58–80 years in women). Concomitant disease states and symptoms were recorded. There were 76 patients with hypertension, 33 patients with diabetes mellitus, and 44 patients with hyperlipidemia. While 57 patients showed ischemic symptoms in the ipsilateral carotid territory, 27 patients exhibited asymptomatic ICA stenosis. None of the patients had an altered level of consciousness or restlessness.

All patients underwent preoperative MR angiography of the cervical arteries. The overall average degree of ICA stenosis was $88.0\% \pm 8.2$, with a range of 70%–99%, as per the North American Symptomatic Carotid Endarterectomy Trial (25). None of the patients had stenosis greater than 70% or occlusion in the contralateral ICA. Institutional review board approval and informed consent were obtained.

Published online

10.1148/radiol.10090930

Radiology 2010; 256:924–931

Abbreviations:

BT = brain temperature
CBF = cerebral blood flow
CEA = carotid endarterectomy
CI = confidence interval
ICA = internal carotid artery
NAA = *N*-acetylaspartate
ROI = region of interest

Author contributions:

Guarantor of integrity of entire study, K.O.; study concepts/study design or data acquisition or data analysis/interpretation, all authors; manuscript drafting or manuscript revision for important intellectual content, all authors; manuscript final version approval, all authors; literature research, T.M., Y.Y., D.I., K.A., K.Y.; clinical studies, T.M., K.O., D.I., M.S., K.K., K.A., M.K., A.O.; statistical analysis, K.O., Y.Y., D.I., H.N., M.K., K.Y.; and manuscript editing, K.O., Y.Y., D.I., M.S., K.K., H.N., A.O.

Authors stated no financial relationship to disclose.

Advances in Knowledge

- A significant correlation was observed between preoperative difference in brain temperature between cerebral hemispheres measured by using proton MR spectroscopy and increases in cerebral blood flow in the affected hemisphere immediately after carotid endarterectomy.
- Elevated preoperative brain temperature difference was significantly associated with the development of postoperative cerebral hyperperfusion.

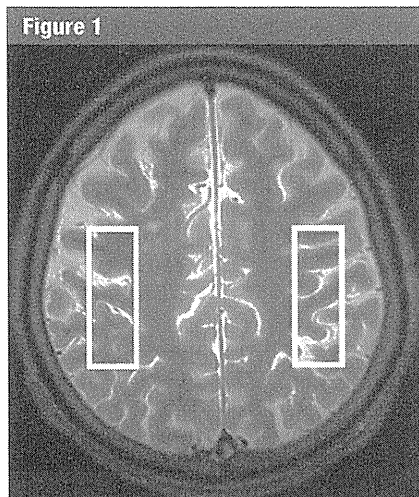


Figure 1: ROIs placed on axial short inversion time inversion-recovery MR image to obtain BT by using MR spectroscopy in 79-year-old man with symptomatic right ICA stenosis (95%) who exhibited hyperperfusion syndrome after CEA. Preoperative Δ BT (BT in affected hemisphere minus BT in contralateral hemisphere) calculated by using the ROIs was +1.15.

BT Measurements at MR Spectroscopy

This study utilized a 3.0-T imager (Signa Excite HD; GE Healthcare, Milwaukee, Wis) with a “birdcage” quadrature head coil. First, all patients underwent axial short inversion time inversion-recovery imaging. From among sections obtained through the centrum semiovale, the section with the thickest white matter was selected. A single-voxel region of interest (ROI) was manually and symmetrically placed in the cerebral cortex parallel to the white matter (Fig 1). Voxel size was $17 \times 50 \times 15 \text{ mm}^3$. Next, acquisition of proton MR spectroscopy data was performed by using point-resolved spectroscopy without water suppression to estimate BT (Fig 2). The following parameters were used: repetition time msec/echo time msec, 2000/144; data size, 4 K; spectral width, 5000 Hz; and 96 acquisitions (3.9 minutes) (24,26,27). During MR spectroscopy, ambient temperature was maintained at $21^\circ\text{--}25^\circ\text{C}$. The MR spectroscopy study was performed within 7 days before CEA.

Raw data from proton MR spectroscopy were transferred to a postprocessing computer (apodization; 1 Hz and

fast Fourier transform), analyzed by using the automatic curve-fitting procedure, and decomposed into Lorentzian peak components by using custom software created in house (24,26,27). In MR spectroscopy, a Lorentzian line shape was commonly assumed on the basis of a one-exponential transverse relaxation behavior of the spins. The real part of the signal was thus used to estimate spectral parameters in a line shape fitting analysis (26). BT for each voxel was calculated from the chemical shift difference between water and NAA signals ($\Delta\text{H}_2\text{O} - \text{NAA}$) by using calibration data from Cady et al and Yoshioka et al (19,27), as follows: T (in degrees Celsius) = $286.9 - 94 \cdot (\Delta\text{H}_2\text{O} - \text{NAA})$, where T is temperature.

The difference between BT in the affected hemisphere and that in the contralateral hemisphere (value in affected hemisphere minus value in contralateral hemisphere) was calculated on each short inversion time inversion-recovery ROI image and was defined as Δ BT.

Prior to the present study, 11 healthy subjects (six men and five women; mean

age, $41 \text{ years} \pm 8$; age range, 20–61 years) were examined by using the same methods to obtain control values. The control value for Δ BT was -0.01 ± 0.25 when the left and right sides were defined as the affected and contralateral sides, respectively.

CBF Measurements at Single Photon Emission Computed Tomography

CBF was assessed by using *N*-isopropyl-*p*- ^{123}I -iodoamphetamine and single photon emission computed tomography (SPECT) performed with a ring-type scanner (Headtome-SET 080; Shimadzu, Kyoto, Japan) before and immediately after CEA. In addition, patients with post-CEA hyperperfusion underwent a third CBF measurement performed in the same manner 3 days after CEA.

The *N*-isopropyl-*p*- ^{123}I -iodoamphetamine SPECT study was performed as described previously (28), and the CBF images were calculated according to the *N*-isopropyl-*p*- ^{123}I -iodoamphetamine autoradiography method (28,29). One tomographic plane through the centrum semiovale was selected for each patient.

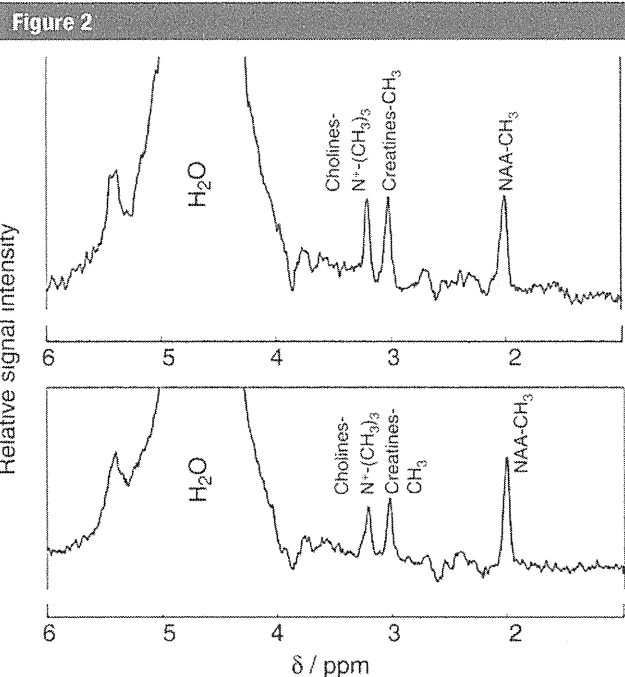


Figure 2: Proton MR spectra obtained by using point-resolved spectroscopy without water suppression in the ROIs in Figure 1. Upper graph: Spectrum in the cerebral hemisphere ipsilateral to that treated with surgery. Lower graph: Spectrum in the contralateral cerebral hemisphere.

One large irregular ROI was manually drawn in the portion of the cerebral cortex perfused by the middle cerebral artery, as per the atlas developed by Kretschmann and Weinrich (30), and the CBF was determined in each ROI. Three SPECT studies were used to analyze identical ROIs in each subject.

Post-CEA hyperperfusion was defined as a CBF increase of 100% or greater (ie, a doubling) compared with preoperative values, as according to Piepgras et al (1).

Intraoperative and Postoperative Management

All patients underwent surgery with general anesthesia. An intraluminal shunt was not used in these procedures. The mean duration of ICA clamping was 36 minutes, ranging from 28 to 48 minutes. A 5000-IU bolus of heparin was administered prior to ICA clamping.

In all patients with post-CEA hyperperfusion, intensive control of arterial blood pressure between 100 and 140 mm Hg was instituted by using intravenous administration of antihypertensive drugs immediately after SPECT. When CBF decreased and hyperperfusion resolved on the 3rd postoperative day, pharmacologic control of blood pressure was discontinued. However, if hyperperfusion persisted, systolic arterial blood pressure was maintained between 100 and 140 mm Hg through pharmacologic methods. When hyperperfusion syndrome developed, the patient was placed in a propofol-induced coma with profound hypotension (systolic arterial blood pressure, <90 mm Hg). The diagnosis of hyperperfusion syndrome required (a) seizure, decrease in level of consciousness, and/or development of focal neurologic signs such as motor weakness and (b) hyperperfusion at SPECT performed after CEA without findings of any additional ischemic lesion at postoperative computed tomography (CT) or T1- and T2-weighted MR imaging.

Statistical Analysis

Descriptive data are expressed as means \pm standard deviations. Correlations between preoperative Δ BT and postoperative CBF increases (CBF calculated

as a percentage of the preoperative value minus 100%) were determined by using a linear regression analysis, a computing regression equation, and a correlation coefficient. The relationship between each variable and the development of post-CEA hyperperfusion at SPECT was evaluated with univariate analysis by using the Mann-Whitney *U* test or the χ^2 test. A multiple statistical analysis of factors related to the development of post-CEA hyperperfusion at SPECT was also performed by using a logistic regression model. Variables with $P < .2$ in the univariate analyses were selected for analysis in the final model. Differences were deemed statistically significant at $P < .05$. The accuracy of preoperative Δ BT for the prediction of post-CEA hyperperfusion at SPECT was determined by using a receiver operating characteristic curve when the relationship between the two was statistically significant. The curve was calculated in increments or decrements of 1 standard deviation from the mean value of Δ BT in healthy subjects. Exact 95% confidence intervals (CIs) of sensitivity, specificity, and positive and negative predictive values were computed by using the binomial distributions.

Results

Eighty-three of the 84 examined patients recovered from surgery without developing new major neurologic deficits. Furthermore, these 83 patients did not exhibit additional ischemic lesions at postoperative CT and MR imaging that included T1- and T2-weighted imaging. The remaining patient, who underwent right CEA, developed a new postoperative neurologic deficit (left hemiparesis) that persisted for more than 24 hours after surgery. MR imaging on the 1st postoperative day revealed infarcts in the cerebral hemisphere ipsilateral to CEA.

Preoperative Δ BT ranged from 1.77 to 1.31. The increase in CBF immediately after CEA ranged from -20% to $+20\%$ when preoperative Δ BT was less than 0 and there was no correlation between the two variables; the increase in CBF ranged from -10% to $+140\%$ when preoperative Δ BT was greater than 0

and a significant linear correlation was observed between the two variables ($r = 0.763$ and $P < .001$) (Fig 3).

Nine patients (11%) met CBF criteria for post-CEA hyperperfusion at SPECT performed immediately after surgery. The patient with a new major postoperative neurologic deficit and new cerebral infarcts in the corresponding hemisphere at postoperative MR imaging did not exhibit post-CEA hyperperfusion at SPECT. Results of univariate analysis of factors potentially related to the development of cerebral hyperperfusion after CEA are summarized in the Table. The preoperative Δ BT was significantly higher in patients with post-CEA hyperperfusion than in those without. Other variables were not significantly associated with the development of post-CEA hyperperfusion. After eliminating closely related variables in the univariate analyses, the following confounders ($P < .2$) were adopted in the logistic regression model for the multiple analysis: age, symptomatic lesion, degree of ICA stenosis, and preoperative Δ BT. Subsequent multivariate analysis revealed that high preoperative Δ BT was significantly associated with the development of postoperative cerebral hyperperfusion ($P = .006$; 95% CI: .001, .155).

Sensitivity and specificity for Δ BT at the cutoff point lying closest to the left upper corner of the receiver operating characteristic curve for the prediction of post-CEA hyperperfusion were 100% (nine of nine; 95% CI: 66%, 100%) and 87% (65 of 75; 95% CI: 77%–93%) (cutoff point = $+0.49$: the mean $+2$ standard deviations of the control value obtained in healthy subjects), respectively (Fig 3). Positive and negative predictive values were 47% (nine of 19; 95% CI: 24%, 71%) and 100% (65 of 65; 95% CI: 94%, 100%), respectively.

Hyperperfusion was not present at the SPECT examination performed on the 3rd postoperative day in seven of the nine patients with hyperperfusion immediately after CEA; these seven patients had uneventful postoperative courses. However, the remaining two patients with cerebral hyperperfusion immediately after CEA experienced persistent hyperperfusion on the 3rd

Risk Factors for Development of Postoperative Cerebral Hyperperfusion at SPECT

Risk Factor	Postoperative Hyperperfusion		P Value
	Yes (n = 9)	No (n = 75)	
Age (y)*	70.2 ± 8.3	67.1 ± 7.4	.148
Male sex	9 (100)	65 (87)	.591
Hypertension	9 (100)	67 (89)	.590
Diabetes mellitus	4 (44)	29 (39)	.733
Hyperlipidemia	3 (33)	41 (55)	.298
Symptomatic lesions	9 (100)	48 (64)	.052
Degree of ICA stenosis (%)*	92.2 ± 5.1	87.5 ± 8.3	.061
Duration of ICA clamping (min)*	35.6 ± 4.2	35.9 ± 5.1	.885
Preoperative ΔBT*	1.03 ± 0.30	-0.09 ± 0.57	<.001

Note.—Unless otherwise specified, data are numbers of patients, with percentages in parentheses.

* Data are means ± standard deviations.

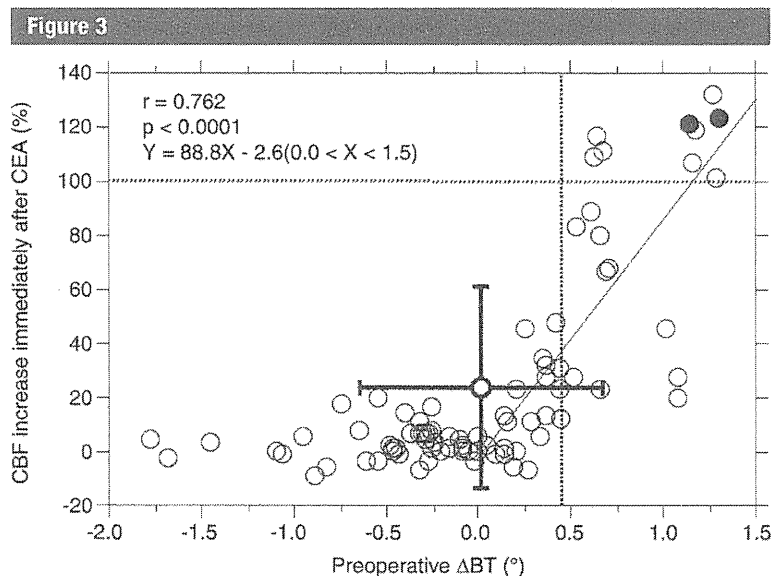


Figure 3: Graph shows correlation between preoperative Δ BT and increase in CBF immediately after CEA. Solid line = function between the two factors, ● = patient who developed hyperperfusion syndrome, horizontal dotted line = CBF increase of 100% (the definition of hyperperfusion), vertical dotted line = mean + 2 standard deviations of Δ BT in healthy subjects, error bar = mean \pm standard deviation of each value.

postoperative day and developed the hyperperfusion syndrome. These two patients experienced confusion and hemiparesis, with onset on the 3rd postoperative day in one patient and on the 4th postoperative day in the second patient. Both patients were placed in a propofol-induced coma. The pre- and postoperative SPECT CBF images in one of these patients are shown in Figure 4. Following termination of the

propofol-induced coma, both patients eventually experienced full recovery.

Discussion

The results of the present study demonstrated that BT, as measured with preoperative proton MR spectroscopy, can help identify patients at risk for post-CEA cerebral hyperperfusion. Although SPECT with an acetazolamide challenge

is a reliable method for predicting cerebral hyperperfusion after CEA (16–18), the clinical use of SPECT is precluded by its high cost and limited availability. In addition, acetazolamide is associated with frequent and various adverse side effects, including metabolic acidosis, hypokalemia, numbness of the extremities, headache, tinnitus, gastrointestinal disturbances, and Stevens-Johnson syndrome (31,32). Studies (15) have demonstrated that measurements of cerebral blood volume at perfusion-weighted MR imaging with gadolinium-based contrast agents also can help identify patients at risk for post-CEA cerebral hyperperfusion. However, contrast agents may be associated with the development of nephrogenic systemic fibrosis in the setting of renal insufficiency (33). Arterial spin labeling and blood oxygen level-dependent imaging are noninvasive MR imaging methods that do not require gadolinium-based contrast agents for perfusion measurement (34,35). However, arterial spin labeling can be used to measure only CBF, and it requires administration of acetazolamide to quantify cerebral perfusion reserve (34). Although blood oxygen level-dependent imaging can help estimate cerebral perfusion reserve (35), whether its findings predict cerebral hyperperfusion after CEA remains unclear. In contrast, the present method does not require administration of radioisotopes or contrast agents and is therefore best suited for clinical use.

Investigators have proposed various mechanisms for the development of post-CEA hyperperfusion (3). In cases of severe ICA stenosis and deficient collateral circulation, hemispheric perfusion pressure is severely reduced distal to the ICA stenosis. This may result in a reduction of perfusion pressure below the compensatory capacity of autoregulatory mechanisms, thus leading to maximal dilatation of resistance vessels and chronic hypoperfusion, or “miserable perfusion.” After normal perfusion pressure is restored by means of CEA, chronically impaired autoregulatory mechanisms may require several days to adjust to the new steady state, resulting in hyperperfusion in the interim. The present

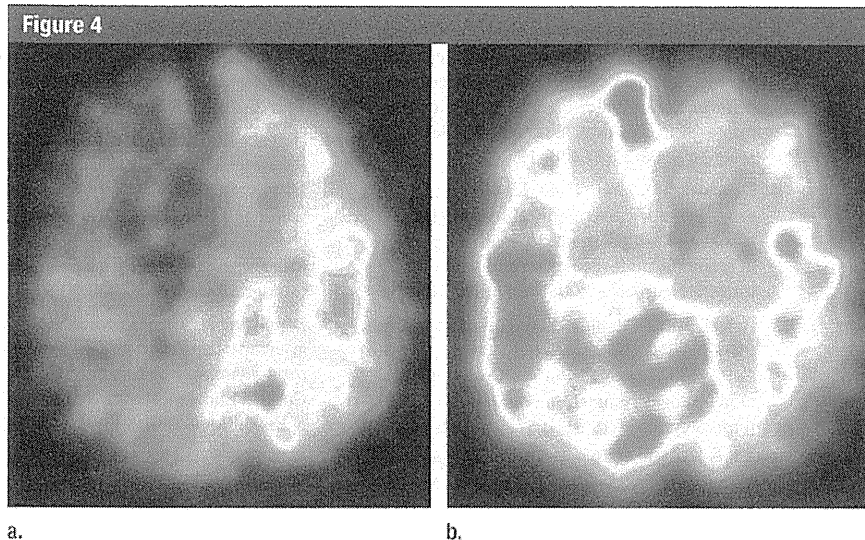


Figure 4: SPECT images in same patient as in Figure 1. (a) Preoperative image shows a decrease in CBF in the right cerebral hemisphere, in which hyperperfusion is observed on (b) image obtained immediately after CEA. This patient developed confusion and left motor weakness 3 days after surgery.

study demonstrated that while there was no correlation between preoperative Δ BT and an increase in CBF immediately after CEA when preoperative Δ BT was less than 0, a significant linear correlation was observed between the two variables when preoperative Δ BT was greater than 0. It also showed that high preoperative Δ BT was the only significant independent predictor of post-CEA hyperperfusion. Because positive and high Δ BT indicates dilation of resistance vessels and misery perfusion in the affected hemisphere (24), our findings support the theory that hyperperfusion results from the loss of normal vasoconstriction secondary to chronic cerebral ischemia and from maladaptive autoregulatory mechanisms.

In the present study, Δ BT had low positive and high negative predictive values for the prediction of post-CEA hyperperfusion; the cutoff point of Δ BT in these values was the mean + 2 standard deviations of the control value obtained in healthy subjects (+0.49°). Furthermore, the cutoff point of Δ BT was identical to that used to detect misery perfusion with a high positive predictive value (24), and the high negative and low positive predictive values in the present study corresponded to previous data obtained by using measurements of cerebrovascular reactivity

to acetazolamide at SPECT (16–18). One group (36) reported that most patients with reduced preoperative cerebrovascular reactivity to acetazolamide and hemispheric hypoperfusion during clamping of the ICA developed post-CEA hyperperfusion, suggesting that, in addition to the impairment of cerebrovascular autoregulation caused by chronic ischemia, intraoperative acute global ischemia contributes to the pathogenesis of post-CEA hyperperfusion. This may account for the low positive predictive value for the prediction of post-CEA hyperperfusion when only preoperative measurement of cerebral hemodynamics was used.

The present study had several limitations. First, this study included only patients with unilateral ICA or middle cerebral artery occlusive disease and used the difference in BT between the affected and unaffected sides to help detect hemodynamic impairment in the affected cerebral hemisphere. However, impairments in cerebral hemodynamics are more severe in patients with bilateral major cerebral artery occlusive disease than in those with unilateral major cerebral artery occlusive disease (37), and whole-brain temperature is affected by body temperature but not by ambient temperature (38). Thus, whether cerebral hemodynamic impairment in

patients with bilateral major cerebral artery occlusive disease can be detected by using the absolute value of BT remains unclear. Second, the cerebral hemisphere with ICA stenosis often exhibits brain atrophy. In that situation, the proportion of cerebrospinal fluid occupying the ROI used for measurement of BT is high. Cerebrospinal fluid in the ROI may reduce the accuracy of brain tissue temperature measured by using MR spectroscopy. The proportion of the white and gray matter occupying the ROI varies in each subject, which may also affect BT measured in the ROI. Third, physiologic brain motion may cause inaccuracies in metabolite concentration measurements with MR spectroscopy (39). However, the point-resolved spectroscopy technique used in the present study is relatively insensitive to physiologic brain motion (39,40). Because our study cohort did not include any subject with an altered level of consciousness or restlessness, the effects of physiologic brain motion on MR spectroscopy may be negligible (40). Last, BT was measured in a single-voxel ROI placed over the cerebral hemisphere. Although a topographic map of BT can be obtained by using a multivoxel method (22), BT values acquired from a single voxel may provide more accurate MR spectroscopic estimation of brain tissue temperature than those acquired from multiple voxels because the distortion of the spectrum resulting from using a multivoxel method is larger than that resulting from using a single-voxel method (41).

In conclusion, results of the present study demonstrated that BT measured at preoperative proton MR spectroscopy can help identify patients at risk for post-CEA cerebral hyperperfusion. On the basis of findings from the present and previous studies (11,12,15–18), we propose a practical clinical algorithm: Patients undergo preoperative BT measurement performed by using the present method; when this method reveals high Δ BT, patients should undergo postoperative CBF assessments to confirm the development of cerebral hyperperfusion. Furthermore, patients with postoperative cerebral hyperperfusion should

undergo intensive control of blood pressure to prevent development of cerebral hyperperfusion syndrome, which may result in intracerebral hemorrhage or persistent cognitive impairment.

References

- Piepgras DG, Morgan MK, Sundt TM Jr, Yanagihara T, Mussman LM. Intracerebral hemorrhage after carotid endarterectomy. *J Neurosurg* 1988;68(4):532-536.
- Sundt TM Jr, Sharbrough FW, Piepgras DG, Kearns TP, Messick JM Jr, O'Fallon WM. Correlation of cerebral blood flow and electroencephalographic changes during carotid endarterectomy: with results of surgery and hemodynamics of cerebral ischemia. *Mayo Clin Proc* 1981;56(9):533-543.
- Bernstein M, Fleming JF, Deck JH. Cerebral hyperperfusion after carotid endarterectomy: a cause of cerebral hemorrhage. *Neurosurgery* 1984;15(1):50-56.
- Solomon RA, Loftus CM, Quest DO, Correll JW. Incidence and etiology of intracerebral hemorrhage following carotid endarterectomy. *J Neurosurg* 1986;64(1):29-34.
- Dalman JE, Beenackers IC, Moll FL, Leusink JA, Ackerstaff RG. Transcranial Doppler monitoring during carotid endarterectomy helps to identify patients at risk of postoperative hyperperfusion. *Eur J Vasc Endovasc Surg* 1999;18(3):222-227.
- Jansen C, Sprengers AM, Moll FL, et al. Prediction of intracerebral haemorrhage after carotid endarterectomy by clinical criteria and intraoperative transcranial Doppler monitoring: results of 233 operations. *Eur J Vasc Surg* 1994;8(2):220-225.
- Ouriel K, Shortell CK, Illig KA, Greenberg RK, Green RM. Intracerebral hemorrhage after carotid endarterectomy: incidence, contribution to neurologic morbidity, and predictive factors. *J Vasc Surg* 1999;29(1):82-87.
- Pomposelli FB, Lamparello PJ, Riles TS, Craighead CC, Giangola G, Imparato AM. Intracranial hemorrhage after carotid endarterectomy. *J Vasc Surg* 1988;7(2):248-255.
- Riles TS, Imparato AM, Jacobowitz GR, et al. The cause of perioperative stroke after carotid endarterectomy. *J Vasc Surg* 1994;19(2):206-214.
- Chida K, Ogasawara K, Suga Y, et al. Postoperative cortical neural loss associated with cerebral hyperperfusion and cognitive impairment after carotid endarterectomy: 123I-iomazenil SPECT study. *Stroke* 2009;40(2):448-453.
- Ogasawara K, Kobayashi M, Suga Y, et al. Significance of postoperative crossed cerebellar hypoperfusion in patients with cerebral hyperperfusion following carotid endarterectomy: SPECT study. *Eur J Nucl Med Mol Imaging* 2008;35(1):146-152.
- Ogasawara K, Yamadate K, Kobayashi M, et al. Postoperative cerebral hyperperfusion associated with impaired cognitive function in patients undergoing carotid endarterectomy. *J Neurosurg* 2005;102(1):38-44.
- Reigel MM, Hollier LH, Sundt TM Jr, Piepgras DG, Sharbrough FW, Cherry KJ. Cerebral hyperperfusion syndrome: a cause of neurologic dysfunction after carotid endarterectomy. *J Vasc Surg* 1987;5(4):628-634.
- Spetzler RF, Wilson CB, Weinstein P, Mehdorn M, Townsend J, Telles D. Normal perfusion pressure breakthrough theory. *Clin Neurosurg* 1978;25:651-672.
- Fukuda T, Ogasawara K, Kobayashi M, et al. Prediction of cerebral hyperperfusion after carotid endarterectomy using cerebral blood volume measured by perfusion-weighted MR imaging compared with single-photon emission CT. *AJNR Am J Neuroradiol* 2007;28(4):737-742.
- Hosoda K, Kawaguchi T, Shibata Y, et al. Cerebral vasoreactivity and internal carotid artery flow help to identify patients at risk for hyperperfusion after carotid endarterectomy. *Stroke* 2001;32(7):1567-1573.
- Ogasawara K, Yukawa H, Kobayashi M, et al. Prediction and monitoring of cerebral hyperperfusion after carotid endarterectomy by using single-photon emission computerized tomography scanning. *J Neurosurg* 2003;99(3):504-510.
- Yoshimoto T, Houkin K, Kuroda S, Abe H, Kashiwaba T. Low cerebral blood flow and perfusion reserve induce hyperperfusion after surgical revascularization: case reports and analysis of cerebral hemodynamics. *Surg Neurol* 1997;48(2):132-138.
- Cady EB, D'Souza PC, Penrice J, Lorek A. The estimation of local brain temperature by in vivo 1H magnetic resonance spectroscopy. *Magn Reson Med* 1995;33(6):862-867.
- Corbett RJ, Laptook A, Weatherall P. Non-invasive measurements of human brain temperature using volume-localized proton magnetic resonance spectroscopy. *J Cereb Blood Flow Metab* 1997;17(4):363-369.
- Jayasundar R, Singh VP. In vivo temperature measurements in brain tumors using proton MR spectroscopy. *Neurol India* 2002;50(4):436-439.
- Karaszewski B, Wardlaw JM, Marshall I, et al. Measurement of brain temperature with magnetic resonance spectroscopy in acute ischemic stroke. *Ann Neurol* 2006;60(4):438-446.
- Nybo L, Secher NH, Nielsen B. Inadequate heat release from the human brain during prolonged exercise with hyperthermia. *J Physiol* 2002;545(pt 2):697-704.
- Ishigaki D, Ogasawara K, Yoshioka Y, et al. Brain temperature measured using proton MR spectroscopy detects cerebral hemodynamic impairment in patients with unilateral chronic major cerebral artery stenosis-occlusive disease: comparison with positron emission tomography. *Stroke* 2009;40(9):3012-3016.
- Beneficial effect of carotid endarterectomy in symptomatic patients with high-grade carotid stenosis. North American Symptomatic Carotid Endarterectomy Trial Collaborators. *N Engl J Med* 1991;325(7):445-453.
- Yoshioka Y, Oikawa H, Ehara S, et al. Non-invasive measurement of temperature and fractional dissociation of imidazole in human lower leg muscles using 1H-nuclear magnetic resonance spectroscopy. *J Appl Physiol* 2005;98(1):282-287.
- Yoshioka Y, Shimada R, Oikawa H, et al. Evaluation of noninvasive measurement of human brain temperature using 1H magnetic resonance spectroscopy at 3T. *J Iwate Med Assoc* 2003;55(5):377-384.
- Ogasawara K, Ito H, Sasoh M, et al. Quantitative measurement of regional cerebrovascular reactivity to acetazolamide using 123I-N-isopropyl-p-iodoamphetamine autoradiography with SPECT: validation study using H2 15O with PET. *J Nucl Med* 2003;44(4):520-525.
- Iida H, Itoh H, Nakazawa M, et al. Quantitative mapping of regional cerebral blood flow using iodine-123-IMP and SPECT. *J Nucl Med* 1994;35(12):2019-2030.
- Kretschmann HJ, Weinrich W. *Neuroanatomy and cranial computed tomography*. New York, NY: Thieme, 1986: 70-74.
- Derick RJ. Carbonic anhydrase inhibitors. In: Mauger TF, Craig EL, eds. *Hevener's ocular pharmacology*. 6th ed. St. Louis, Mo: Mosby, 1994.
- Ogasawara K, Tomitsuka N, Kobayashi M, et al. Stevens-Johnson syndrome associated with intravenous acetazolamide administration for evaluation of cerebrovascular reactivity: case report. *Neurol Med Chir (Tokyo)* 2006;46(3):161-163.
- Wiginton CD, Kelly B, Oto A, et al. Gadolinium-based contrast exposure, nephrogenic systemic fibrosis, and gadolinium detection in tissue. *AJR Am J Roentgenol* 2008;190(4):1060-1068.
- Zappe AC, Reichold J, Burger C, et al. Quantification of cerebral blood flow in non-human primates using arterial spin labeling and a two-compartment model. *Magn Reson Imaging* 2007;25(6):775-783.

35. Shiino A, Morita Y, Tsuji A, et al. Estimation of cerebral perfusion reserve by blood oxygenation level-dependent imaging: comparison with single-photon emission computed tomography. *J Cereb Blood Flow Metab* 2003;23(1):121-135.
36. Komoribayashi N, Ogasawara K, Kobayashi M, et al. Cerebral hyperperfusion after carotid endarterectomy is associated with preoperative hemodynamic impairment and intraoperative cerebral ischemia. *J Cereb Blood Flow Metab* 2006;26(7):878-884.
37. Reinhard M, Müller T, Roth M, Guschlbauer B, Timmer J, Hetzel A. Bilateral severe carotid artery stenosis or occlusion - cerebral autoregulation dynamics and collateral flow patterns. *Acta Neurochir (Wien)* 2003;145(12):1053-1059.
38. Shiraki K, Sagawa S, Tajima F, Yokota A, Hashimoto M, Brengelmann GL. Independence of brain and tympanic temperatures in an unanesthetized human. *J Appl Physiol* 1988;65(1):482-486.
39. Pattany PM, Massand MG, Bowen BC, Quencer RM. Quantitative analysis of the effects of physiologic brain motion on point-resolved spectroscopy. *AJNR Am J Neuroradiol* 2006;27(5):1070-1073.
40. Katz-Brull R, Lenkinski RE. Frame-by-frame PRESS 1H-MRS of the brain at 3 T: the effects of physiological motion. *Magn Reson Med* 2004;51(1):184-187.
41. Childs C, Hiltunen Y, Vidyasagar R, Kauppinen RA. Determination of regional brain temperature using proton magnetic resonance spectroscopy to assess brain-body temperature differences in healthy human subjects. *Magn Reson Med* 2007;57(1):59-66.

Simple Assessment of Cerebral Hemodynamics Using Single-Slab 3D Time-of-Flight MR Angiography in Patients with Cervical Internal Carotid Artery Steno-Occlusive Diseases: Comparison with Quantitative Perfusion Single-Photon Emission CT

ORIGINAL RESEARCH

R. Hirooka
K. Ogasawara
T. Inoue
S. Fujiwara
M. Sasaki
K. Chida
D. Ishigaki
M. Kobayashi
H. Nishimoto
Y. Otawara
E. Tsushima
A. Ogawa

BACKGROUND AND PURPOSE: Visualization of the peripheral arteries on single-slab 3D time-of-flight (TOF) MR angiography (MRA) can reflect blood flow velocity. The velocity in the middle cerebral artery (MCA) may correlate with cerebrovascular reactivity (CVR) to acetazolamide, which can be used to assess hemodynamic impairment. The goal of this study was to compare the signal intensity of the MCA on MRA versus CVR quantified by perfusion single-photon emission CT (SPECT).

MATERIALS AND METHODS: The signal intensity of the MCA on single-slab 3D time-of-flight MRA was graded according to the ability to visualize the MCA in 108 cerebral hemispheres of 87 patients with unilateral or bilateral cervical internal carotid artery (ICA) steno-occlusive diseases. SPECT-CVR was also calculated by measuring cerebral blood flow before and after acetazolamide challenge. Ten healthy subjects were studied to obtain control SPECT-CVR values. All subjects provided written informed consent before the study.

RESULTS: CVR was significantly lower in cerebral hemispheres with reduced MCA signal intensity than in those with normal intensity ($P < .05$). When the reduced signal intensity of the MCA on MRA was defined as abnormal, and when a CVR less than the mean $- 2$ SD of healthy subjects was defined as reduced, MRA grading resulted in a 86.2% sensitivity and 69.6% specificity, with 51.0% positive-predictive and 93.2% negative-predictive values to detect reduced CVR.

CONCLUSIONS: This simple MRA method can assess hemodynamic impairment with a high negative-predictive value.

As local cerebral perfusion pressure falls, regional cerebral blood flow is maintained by the cerebrovascular autoregulatory mechanisms of precapillary resistance vessel dilation.^{1,2} Some vasodilatory property of vessels can be detected by measurement of cerebral blood flow at rest and after a vasodilatory stimulus, such as inhalation of carbon dioxide or administration of acetazolamide.^{3,4} Quantitative assessment of cerebrovascular reactivity (CVR) to acetazolamide can be used to assess the severity of hemodynamic impairment in patients with major cerebral artery occlusive disease.^{5,6} In fact, recent prospective studies have demonstrated that reduced CVR after acetazolamide administration can predict the risk for stroke recurrence in patients with symptomatic internal carotid artery (ICA) occlusive disease.⁷⁻⁹ Furthermore, patients with reduced CVR are at increased risk for cerebral hyperperfusion after carotid endarterectomy,^{10,11} which may result in intracerebral hemorrhage or cognitive impairment.¹²⁻¹⁴

Measurement of cerebral mean transit time is a sensitive method to estimate CVR to acetazolamide.¹⁵ Specifically, increased mean transit time values correlate with decreased CVR

to acetazolamide, as determined by brain perfusion single-photon emission CT (SPECT).^{16,17} The cerebral mean transit time is also proportional to blood flow velocity in the middle cerebral artery (MCA).^{18,19} Thus, the MCA blood flow velocity may identify reduced CVR to acetazolamide.

MR angiography (MRA) with use of 3D time-of-flight (TOF) uses signals generated by the inflow of fresh, unsaturated, and fully magnetized blood spins into the slab.^{20,21} These spins are gradually saturated during movement within the slab. This saturation effect causes signal intensity loss in the peripheral arteries. The signal intensity loss from the saturation effect is flow velocity dependent and is more pronounced with lower flow velocity,²² particularly in single-slab 3D TOF MRA.²¹

The goal of our study was to compare the usefulness of MCA signal intensity on single-slab 3D TOF MRA versus CVR to acetazolamide measured by quantitative perfusion SPECT for the detection of cerebral hemodynamic impairment in patients with cervical ICA steno-occlusive diseases.

Materials and Methods

Patients

This study included 87 patients (3 women and 84 men) aged 52 to 81 years (mean age, 68 years) with steno-occlusive diseases in the cervical portion of the ICA. None of the patients had altered level of consciousness, restlessness, dementia, or cardiac failure. All patients underwent MRA at local hospitals with use of a 1.5T or less imager,

Received June 12, 2008; accepted after revision September 26.

From the Advanced Medical Research Center (R.H., T.I., S.F., M.S., D.I., H.N.) and Department of Neurosurgery (K.O., K.C., M.K., Y.O., A.O.), Iwate Medical University, and Graduate School of Health Sciences (E.T.), Hirosaki University, Japan.

Please address correspondence to Kuniaki Ogasawara, MD, Department of Neurosurgery, Iwate Medical University, Uchimarui, 19-1, Morioka 020-8505, Japan; e-mail: kuogasa@iwate-med.ac.jp

DOI 10.3174/ajnr.A1389

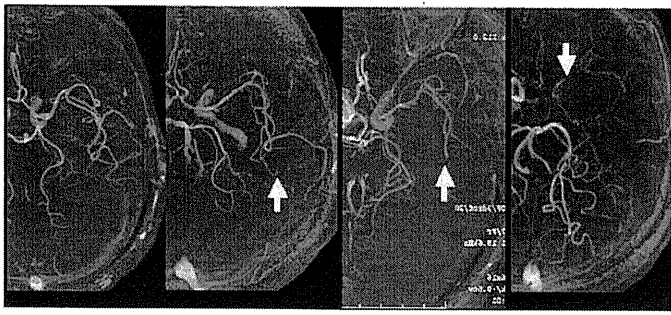


Fig 1. Degree of visualization of the ipsilateral MCA on brain MRA was graded as follows: all M3 branches of the left MCA could be visualized to the cortical surface (*grade A*), one M3 branch could not be visualized to the cortical surface (*grade B*, *arrow*), one M2 branch could not be visualized along its course (*grade C*, *arrow*), and the M1 could not be visualized along its course (*grade D*, *arrow*).

which revealed preexisting lesions in all cases. Patients diagnosed with Moyamoya disease on MRA were excluded from our study. As per the North American Symptomatic Carotid Endarterectomy Trial,²³ cervical MRA at our department with a 3T imager demonstrated more than 70% unilateral ICA stenosis in 60 patients, unilateral ICA occlusion in 6 patients, bilateral ICA stenoses in 19 patients, bilateral ICA occlusions in 1 patient, and unilateral ICA stenosis and contralateral ICA occlusion in 1 patient. Thus, this study included 108 cerebral hemispheres with ipsilateral cervical ICA steno-occlusive diseases and 66 cerebral hemispheres without lesions. Of cerebral hemispheres with lesions, 66 were associated with ischemic symptoms. Furthermore, transient ischemic attacks were present in 36 cerebral hemispheres, including 16 cerebral hemispheres with definite cerebral infarction and 20 cerebral hemispheres without definite cerebral infarction on conventional MR imaging. The remaining 30 cerebral hemispheres had minor complete strokes with definite cerebral infarction on MR imaging.

The study protocol was approved by the local ethics committee. All patients provided written informed consent before the study.

MRA Study

MRA was performed with a 3T imager (Signa Excite HD; GE Healthcare, Milwaukee, Wis). Axial single-slab 3D TOF MRA in the cervical portion was obtained at the carotid bifurcation with use of 5-inch surface coils (TR, 21 ms; TE, 3 ms; variable flip angle, 17–34° in the inferosuperior direction; matrix size, 512 × 256; FOV, 22 cm; section thickness, 1.2 mm; partition size, 60 with zero-fill interpolation [120 sections with 0.6-mm intervals]; NEX, 1; presaturation pulse above the slab, a fat suppression pulse, and a flow compensation; and acquisition time, 4 minutes 26 seconds). Then, axial single-slab 3D TOF MRA of the intracranial arteries, which was parallel to the anterior/posterior commissure line and was covered from the pontomedullary junction to the corpus callosum, was obtained with use of an 8-channel head coil (TR, 30 ms; TE, 3.7 ms; variable flip angles of 17–34° in the inferosuperior direction; matrix size, 512 × 320; FOV, 24 cm; section thickness, 1.0 mm; partition size, 90 with zero-fill interpolation [180 sections with 0.5-mm intervals]; NEX, 1; magnetization transfer pulse and flow compensation; and acquisition time, 6 minutes 22 seconds).

Signal intensity of the MCA in the intracranial MRA was visually classified into the following 4 grades according to the ability to visualize the MCA (Fig 1): all M3 branches of the MCA could be visualized to the cortical surface (*grade A*), 1 or more M3 branches could not be visualized to the cortical surface (*grade B*), 1 or more M2 branches

could not be visualized along its course (*grade C*), and the M1 could not be visualized along its course (*grade D*).

To assess interobserver variability of the MRA grading, 2 experienced neuroradiologists independently reviewed all MRA images (first, R.H.; and second, T.I.). In addition, the first observer reviewed the same images a second time, after a 3-month interval to account for the intraobserver variability of the study. Both observers were blinded to all patient information other than the images to be reviewed. Each observer was blind to the other's assessments and to their own previous assessments.

SPECT Study

Brain perfusion was assessed with use of iodine 123 *N*-isopropyl-p-iodoamphetamine (¹²³I-IMP) and SPECT. We performed SPECT studies using a ring-type SPECT scanner, a Headtome-SET080 (Shimadzu, Kyoto, Japan), which provides 31 tomographic images simultaneously. The spatial resolution of the scanner with a low-energy, all-purpose collimator was 13 mm full width at half maximum (FWHM) at the center of the FOV, and the section thickness was 25 mm FWHM at the FOV center. Image sections were taken at 5-mm center-to-center spacing parallel to the orbitomeatal line. We reconstructed the images using the weighted-filtered backprojection technique, in which the attenuation correction was made by detecting the edge of the object. An attenuation coefficient of 0.065 cm⁻¹, a Butterworth filter (cutoff point, 0.45 cycle/cm; order, 3) and a ramp filter were used for image reconstruction.

The ¹²³I-IMP SPECT studies at the resting state and with acetazolamide challenge were performed as described previously.²⁴ The cerebral blood flow images were calculated according to the ¹²³I-IMP-autoradiography method.^{24,25} The same standard input function at the resting state was used in the calculation of cerebral blood flow with acetazolamide challenge. The V_d value was assumed to be 35 mL/mL in the calculation of cerebral blood flow images.

We transformed all SPECT images into the standard brain size and shape by linear and nonlinear transformation using SPM99 for anatomic standardization.²⁶ Thus, the brain images of all subjects had the same anatomic format. Next, 318 constant regions of interest (ROIs) were automatically placed in both the cerebral and cerebellar hemispheres with a 3D stereotaxic ROI template.²⁷ The ROIs were grouped into 10 segments (callosomarginal, pericallosal, precentral, central, parietal, angular, temporal, posterior, hippocampus, and cerebellum) in each hemisphere according to the arterial supply. Only 5 (precentral, central, parietal, angular, and temporal) of these 10 segments were summed and defined as an ROI perfused by the MCA (Fig 2). The mean cerebral blood flow value at the resting state and with acetazolamide challenge was measured in each MCA ROI. Then, CVR to acetazolamide was calculated as follows: $CVR (\%) = [(acetazolamide\ challenge\ cerebral\ blood\ flow - resting\ cerebral\ blood\ flow) / resting\ cerebral\ blood\ flow] \times 100$.

Using the same method, we studied 10 healthy subjects (8 men and 2 women; age, 35–65 years; mean age, 52.3 years) to obtain control values.²⁴ The control values of CVR were $36.8 \pm 9.2\%$, respectively. When the values of CVR were less than the mean minus 2 SD (ie, 18.4%), they were rated as reduced CVR. All MRA and SPECT studies were performed within 5 days.

Statistical Analysis

To determine the interobserver and intraobserver agreement of the MRA grading, we calculated the proportion of concordant assessments and κ statistics using data determined by the 2 observers. The